

Journal of King Saud University - Science

Editor-in-Chief

Prof. Omar M. Al-Dossary
Department of Physics and Astronomy
College of Science
King Saud University
P.O. Box 2455, Riyadh 11451
Tel.: 00966 -11-4676378 (secretary)
Fax: 00966 11 4673656
E-mail: omar@ksu.edu.sa

Associate Editors

Prof. Ahmad H. Alghamdi
Chemistry Department,
College of Science
King Saud University
P.O. Box 2455,
Riyadh 11451
Saudi Arabia
Tel.: 966-11-4676001
Fax: 966-11-4675992
E-mail: HYPERLINK "mailto:ahghamdi@ksu.edu.saEditor" ahghamdi@ksu.edu.sa

Prof. Abdullah M.S. Al-Amri
Geology and Geophysics Department
College of Science
King Saud University
Saudi Arabia
E-mail: amsamri@ksu.edu.sa

Prof. Omar M. Al-Dossary
Physics and Astronomy Department
College of Science
King Saud University
Saudi Arabia
E-mail: Omar@ksu.edu.sa

Dr. Amal Abdulaziz Al-Hazzani
Botany and Microbiology Department
College of Science, King Saud University
Saudi Arabia
E-mail: alhazzani@ksu.edu.sa

Prof. Yousef A. Alkhamees
Mathematics Department, College of Science
King Saud University
Saudi Arabia
E-mail: ykhamees@ksu.edu.sa

Dr. Giovanni Benelli
Department of Agriculture, Food and
Environment
University of Pisa, Italy
E-mail: g.benelli@sssup.it; benelli.giovanni@gmail.com

Prof. Demosthenes Ellinas
School of Electronics and Computer
Engineering
Technical University of Crete
Greece
E-mail: ellinas@ece.tuc.gr

Prof. Jun Ling
Department of Basic Sciences
The Commonwealth Medical College, Scranton
USA
E-mail: jling@tcmc.edu

Prof. Hatem Odah
National Research Institute of Astronomy
and Geophysics
Cairo, Egypt
E-mail: hatemodah@yahoo.com

Prof. Hari M. Srivastava
Department of Mathematics and Statistics
University of Victoria
Canada
E-mail: harimsri@math.uvic.ca

International Advisory Editors

Dr. Marilena Carbone
Universita degli Studi di Roma Tor Vergata,
Roma, Italy

Prof. Asantha Cooray
University of California, Irvine
Department of Physics & Astronomy,
4186 Frederick Reines Hall
Irvine, CA 92697-4575
Tel.: +1 949 824-6832

Dr. G. Dyke
Department of Evolutionary Zoology, University of Debrecen,
Debrecen, Egyetem ter 1., 4032, Hungary

Rizwan Irshad
Ministry of Climate Change, G-5, Islamabad, Pakistan

Prof. X.J. Yang
Department of Mathematics and Mechanics
China University of Mining and Technology
Xuzhou 221008, China

HOSTED BY



Contents lists available at ScienceDirect

Journal of King Saud University – Science

journal homepage: www.sciencedirect.com

Original article

The role of lime juice in improving the performance of basic sites on activated carbon surfaces in sulfate ion adsorption in seawater

Yurida Ekawati^{a,c,*}, I.N.G. Wardana^{a,*}, Oyong Novareza^b, Putu Hadi Setyarini^a, Rokiy Alfanaar^d^a Department of Mechanical Engineering, Brawijaya University, JL. Mayjen Haryono 167, Malang 65145, Indonesia^b Department of Industrial Engineering, Brawijaya University, JL. Mayjen Haryono 167, Malang 65145, Indonesia^c Department of Industrial Engineering, Ma Chung University, Villa Puncak Tidar N-1, Malang 65151, Indonesia^d Department of Chemistry, Palangka Raya University, Jl. Yos Sudarso 73111, Palangka Raya 74874, Indonesia

ARTICLE INFO

Article history:

Received 25 August 2022

Revised 5 June 2023

Accepted 23 June 2023

Available online 28 June 2023

Keywords:

Sulfate

Seawater

Lime juice

Activated carbon

Basic functionalities

ABSTRACT

The aim of this research was to investigate the utilization of lime juice in enhancing the performance of commercially produced activated carbon from coconut shells for decreasing the sulfate ion content in seawater. Seawater, which serves as the raw material for sea salt production, contains relatively high levels of sulfate ions as impurities. The removal of sulfate ions from seawater is essential in minimizing impurities during the crystallization process of sea salt. The study employed two types of activated carbon: activated carbon without further treatment (ACB) and acid-washed activated carbon (ACA). The objective was to explore the mechanism of sulfate ion adsorption when lime juice was introduced to the seawater. Various concentrations of lime juice were used in the adsorption experiment, based on the optimum dosages and time determined in the preliminary study. The results indicated that ACB exhibited a higher sulfate ion adsorption capacity ($320 \text{ mg SO}_4^{2-} \text{ g}^{-1}$) compared to ACA ($298 \text{ mg SO}_4^{2-} \text{ g}^{-1}$). The addition of lime juice led to a decrease in solution pH and an increase in sulfate ion adsorption. This suggests that lime juice enhanced the capacity of basic sites present in the activated carbon. The proposed model for sulfate ion adsorption posits that the ions are attracted to the functional groups and subsequently to the basic sites in the carbon basal planes, mediated by hydronium ions.

© 2023 The Author(s). Published by Elsevier B.V. on behalf of King Saud University. This is an open access article under the CC BY-NC-ND license (<http://creativecommons.org/licenses/by-nc-nd/4.0/>).

1. Introduction

Indonesia, being surrounded by seas and oceans, possesses a significant advantage in sea salt production due to the abundant availability of seawater. However, the quality of sea salt is a concern, and impurities play a crucial role in determining its quality. Impurities such as CaSO_4 (0.5%–1%), MgCl_2 (0.3%–1%), and MgSO_4 (0.2%–0.6%) are commonly found in sea salt (Sedivy, 2009). These impurities originate from various ions present in seawater, including chloride, sodium, sulfate, magnesium, calcium, and potassium (Byrne, 2020). The presence of impurities in sea salt often leads

to higher purification costs compared to the actual cost of the salt itself (Sedivy, 2009). These impurities can be found on both the surface and within the salt crystals (Masuzawa, 1980). The most challenging aspect lies in the refining process of the salt, as the impurities tend to be embedded within the crystal structure.

Additionally, the presence of impurities in salt contributes to moisture absorption and can diminish its saltiness, potentially leading to increased salt consumption, which can have adverse health effects (Heydarieh et al., 2020). Calcium sulfate, in its insoluble form, precipitates in food, causing undesirable visual effects. Moreover, the presence of calcium sulfate increases the risk of stomach cancer (Wong, 2016). Both calcium sulfate and magnesium sulfate are impurities found in sea salt, originating from the high sulfate content present in seawater (Byrne, 2020). It is plausible that by reducing the sulfate content in seawater before its evaporation and crystallization into salt, the occurrence of sulfate salt impurities in sea salt can be minimized.

Numerous investigations have been conducted on the removal of sulfate from aqueous solutions using activated carbon, as evidenced by studies conducted by Hosseini et al. (2017), Hong et al. (2017), and Rahmati et al. (2019). Activated carbon is

* Corresponding authors at: Department of Mechanical Engineering, Brawijaya University, JL. Mayjen Haryono 167, Malang 65145, Indonesia (Y. Ekawati).

E-mail addresses: yurida.ekawati@gmail.com (Y. Ekawati), wardana@ub.ac.id (I.N.G. Wardana).

Peer review under responsibility of King Saud University.



Production and hosting by Elsevier

commonly employed due to its cost-effectiveness and environmentally friendly nature as a method for sulfate removal. Several factors have been identified to influence the adsorption of sulfate onto activated carbon, including the type of activated carbon (Hong et al., 2017), pore volume (Hong et al., 2014), pH, activated carbon dosage, and contact time (Zhu et al., 2019), initial sulfate ion concentration (Runtti et al., 2016), and the surface characteristics of the carbon material (Rahmati et al., 2019). Acidic conditions have been found to enhance sulfate adsorption onto activated carbon, as supported by the research conducted by Runtti et al. (2016) and Rahmati et al. (2019).

Lowering the pH can be achieved by incorporating natural organic ingredients, such as limes or lemons, which are readily accessible in the environment. Limes, specifically, are recognized for their remarkable acidity among various citrus fruits (Berry, 2003). They are extensively cultivated in tropical regions like Indonesia and are available year-round, as they are not limited to a specific season. In addition to containing essential minerals like copper and iron, limes possess a low pH level (Waghaye et al., 2019). The acidity of lime juice can be attributed to the presence of citric acid, a weak organic acid that can significantly impact the pH of a solution. The concentration of citric acid in limes is approximately 0.30 mol/L (Penniston et al., 2008).

The primary aim of this study was to investigate the potential of lime juice in enhancing the adsorption capacity of commercially available activated carbon derived from coconut shells for decreasing sulfate ion levels in seawater. The activated carbon used in this research was in its original form without any additional modifications. Coconut shells are abundantly available and cost-effective raw materials in tropical countries like Indonesia, offering a viable source for the production of activated carbon with diverse applications. Moreover, a conceptual model illustrating the adsorption mechanism of sulfate ions on activated carbon in the presence of lime juice was proposed. This study serves as a foundational investigation, providing insights for future advancements in mitigating impurities in sea salt production through the reduction of impurities in seawater.

2. Material and method

2.1. Material preparation

Seawater samples were collected from a coastal area in Malang, East Java, Indonesia, specifically from the southern beach. The collected seawater was carefully stored in glass containers and kept in a dark and cool environment. Granular activated carbon, obtained from Java Carbon located in Mojokerto, East Java, Indonesia, was utilized without any additional treatments. The activated carbon particles had a size range of 0.60 to 2.36 mm. The production of activated carbon involved the steam activation method. Two variants of activated carbon, namely activated carbon (ACB) and acid-washed activated carbon (ACA), were sourced from the company for the experimental investigation. Lime juice was extracted from locally available green limes. Green limes were preferred due to their higher acidity levels, as the acidity tends to decrease with the aging process of limes (Rangel et al., 2011).

2.2. Material characterization

The seawater samples were subjected to comprehensive analysis to determine the concentrations of various ions. Inductively Coupled Plasma-Optical Emission Spectroscopy (ICP-OES) was employed to measure the levels of magnesium, potassium, sodium, boron, and calcium ions. Nitrate, sulfate, and phosphate ions were quantified using a spectrophotometer, while chloride ions were

determined using argentometry. The surface functional groups present on the activated carbons were characterized using Fourier Transform Infrared (FT-IR) spectroscopy in the spectral range of 450–4000 cm^{-1} . The surface textures of the activated carbons and the presence of specific elements of interest were evaluated using Scanning Electron Microscopy Energy Dispersive X-ray Analysis (SEM EDAX). The specific surface areas of the activated carbons were estimated using the multipoint Brunauer-Emmett-Teller (BET) equation, and the pore diameters were determined using the Barrett-Joyner-Halenda (BJH) method. To assess the pH of the activated carbon, 0.1 g of activated carbon was boiled in 100 ml of distilled water for 5 min. The resulting solution was diluted with distilled water to a final volume of 200 ml, cooled to room temperature, and then measured using a pH meter.

2.3. Adsorption experiments

2.3.1. Adsorption experiment for dosage and time

A preliminary experiment was conducted to determine the optimum activated carbon dosage and adsorption time. The dosage of activated carbons was 30, 40, 50, and 60 mg. Adsorption times varying from 5 min, 1 h, 5 h, and 24 h were used to determine the optimum adsorption time as the equilibrium adsorption time. First, the seawater was filtered using filter paper Whatman No 1 to avoid any interference by the deposit, and 25 ml of the water was put into a 30 ml glass vial. The activated carbons were then added to the seawater and shaken using a rotary shaker at 300 rpm at room temperature (25 – 26 °C) for a particular time. After being shaken and allowed to stand for half an hour, the solutions were filtered using a 0.45 μm nylon filter. Seawater without any treatment was also filtered using a 0.45 μm nylon filter as a control. The sulfate concentration was measured based on the National Standardization of Indonesia method (SNI 6989.20_2009) using a UV-Vis spectrophotometer (Shimadzu, Japan), and the amount of sulfate ion removal was calculated.

Based on the preliminary experiment, the optimum activated carbons' dosages were 40 mg for ACA and 50 mg for ACB, and the equilibrium adsorption time was 1 h. Therefore, these dosages and time were selected to study the effect of added lime juice concentration on sulfate ion adsorption on activated carbons.

2.3.2. Adsorption experiment with lime juice

The dosages of 40 and 50 mg were used for both types of activated carbon to thoroughly examine the effect of adding lime juice to increase the capacity of activated carbon in the adsorption of sulfate ions. In addition, a dosage of 60 mg was included in the experiment to see the effect of increasing the dosage of activated carbon on sulfate adsorption when lime juice was added to the seawater.

Lime juice from local green limes was extracted using a micro-pipette of as much as 20 μl . The juice was added with distilled water to a volume of 10 ml and mixed manually. Seawater without being filtered with the volume of 50 ml was put into a 100 ml glass container. The lime juice solution was mixed with the seawater and shaken with a rotary shaker to make a homogenous solution. The various lime juice of 0, 20, 30, 40, 50, 60, 75, and 100 μl was used for this experiment. The solution was then filtered using a paper filter Whatman No. 1. The pH of the solution was then taken using Ohaus Starter 300 pH meter. For each lime juice concentration, the solution was taken 25 ml each for the two-type activated carbon and put into a 30 ml glass vial. The seawater mix with lime juice was added to the activated carbon and shaken in a rotary shaker at 300 rpm and room temperature for 1 h. After being shaken and allowed to stand for half an hour, the solutions were filtered using a 0.45 μm nylon filter. The sulfate concentration was determined using UV-Vis spectrophotometer (Shimadzu, Japan). The

amount of sulfate ion adsorbed per unit weight of activated carbon, Q_e ($\text{mg SO}_4^{2-} \text{ g}^{-1}$), was calculated using Eq. (1).

$$Q_e = \frac{C_0 - C_e}{m} \times V \quad (1)$$

C_0 = initial sulfate concentration (mg/L).

C_e = sulfate concentration at equilibrium time (mg/L).

m = mass of activated carbon (g).

V = volume of solution (L).

2.4. Statistical analysis

For the preliminary study, triplication was used, and the average amount of sulfate ion removal was calculated. The adsorption experiment with lime juice also used triplication, and the average sulfate ion adsorbed per unit weight of activated carbon was calculated. The triplication used different lime fruits.

3. Result and discussion

3.1. Composition of the seawater

The seawater used in the experiment was stored under appropriate conditions and was not subjected to any additional treatments. Table 1 presents the composition of primary ions found in the seawater. The presence of these ions posed a challenge for sulfate ion adsorption onto activated carbon, as the various ions present in seawater can compete for adsorption sites. To assess the adsorption potential of sulfate ions, the concept of hydration ratio, as proposed by Li et al. (2016), was utilized. Table 2 provides the hydration ratios of commonly encountered ions in seawater, based on the work of Nightingale (1959). From the data, it can be observed that sulfate ions have a lower hydration ratio compared to other ions in seawater, with the exception of nitrate ions. Consequently, there is a potential for the adsorption of sulfate ions from seawater onto activated carbon, as sulfate ions exhibit higher electrostatic selectivity than most other ions.

3.2. Adsorption of sulfate ion in the seawater

Fig. 1 depicts the adsorption results obtained from the experiment. When lime juice was not added, both activated carbon types exhibited relatively low adsorption amounts of sulfate ions at a dosage of 40 mg. Increasing the activated carbon dosage to 50 mg resulted in an increase in sulfate adsorption for ACB, while a decrease was observed for ACA. However, when the dosage was further increased to 60 mg, no significant change in sulfate ion adsorption was observed for either activated carbon type. The presence of various ions in seawater, as indicated in Table 1, created a competitive environment for sulfate ion adsorption on activated carbon. The high concentrations of ions such as sodium, chloride, and magnesium in seawater (Table 1) contributed to the competition for adsorption sites, thereby limiting the adsorption of sulfate ions. Additionally, the relatively high pH of the seawater (Table 1) may have also influenced the adsorption process. It is known that at higher pH levels, activated carbon tends to exhibit better adsorption of cations rather than anions (di Natale et al.,

2008). These factors likely contributed to the relatively low adsorption amounts observed in the absence of lime juice.

The highest adsorption amount when lime juice was added occurred in the dosage of 50 mg. Adding lime juice increased the adsorption amount of sulfate ions for both ACA and ACB. In ACA, the highest adsorption amount was at the lime concentration of 30 μL , while in ACB, the highest sulfate adsorption amount was at a lime concentration of 50 μL . In ACB, increasing the dosage of activated carbon and the concentration of lime juice increased the adsorption amount of sulfate ions. The adsorption amount of ACB was higher than ACA for most of the lime juice concentrations. The highest adsorption capacity of sulfate ions in ACB was 320 $\text{mg SO}_4^{2-} \text{ g}^{-1}$, and in ACA, 298 $\text{mg SO}_4^{2-} \text{ g}^{-1}$.

The experiment showed that ACB performed better than ACA in all the dosages of activated carbon used. Further analysis of the characteristics of the activated carbons needs to be done to understand the phenomenon and how the adsorption mechanism occurs in activated carbons.

3.3. Physical characteristics of the activated carbons

The physical properties of activated carbons, the specific surface area, and pore size, determine the adsorption capacity of the activated carbon (Sun et al., 2018). The morphology of activated carbon is influenced by the method of activating the carbon material (Guan et al., 2018). The carbon used in this experiment was activated by the steam method. The method formed pores and introduced oxygen-containing functional groups (Shen et al., 2008). ACA has activated carbon with acid-washed treatment. The treatment reduced the ash content, lowered the pH, and improved the hydrophilic surface of the activated carbon (Koehlert, 2017). The pH of ACA is lower than ACB (Table 3). Therefore, it can be predicted that ACB had higher basicity than ACA. The ash content of ACB is higher than ACA (Table 3). It can be seen from Fig. 2 that ACA looked cleaner than ACB as the inorganic impurities were lessened. Although there is an indication that ash content affects carbon basicity, it is not clear what effect ash content has on adsorption capacity (Gaya et al., 2015; Miyazato et al., 2020).

Based on Table 3, the average pore size of both types of AC was micropores because the size was less than 2 nm (Ilomuanya et al., 2017). Micropores are effectively used for the adsorption of small molecules, usually between 0.4 nm and 0.9 nm (Álvarez-Merino et al., 2005). The sulfate ion radius is 0.29 nm (Table 2), much smaller than the average pore size of the activated carbons.

Table 3 and Fig. 2 showed that the average pore size of ACA was smaller than ACB. However, ACA had a higher surface area and pore volume than ACB. The difference in physical characteristics of both activated carbons was apparently not significant. ACA had slightly better physical characteristics than ACB but based on the experiment, ACB showed better sulfate ion adsorption than ACA. Even without adding lime juice, ACB performed better than ACA in sulfate ions removal. Therefore, physical characteristics did not seem to influence the adsorption capacity significantly.

3.4. Basic functionalities of the activated carbons

The adsorption of ions from an aqueous solution, such as seawater, relies on the electrostatic interaction between the adsorbate (ions) and the adsorbent (activated carbon). This interaction is

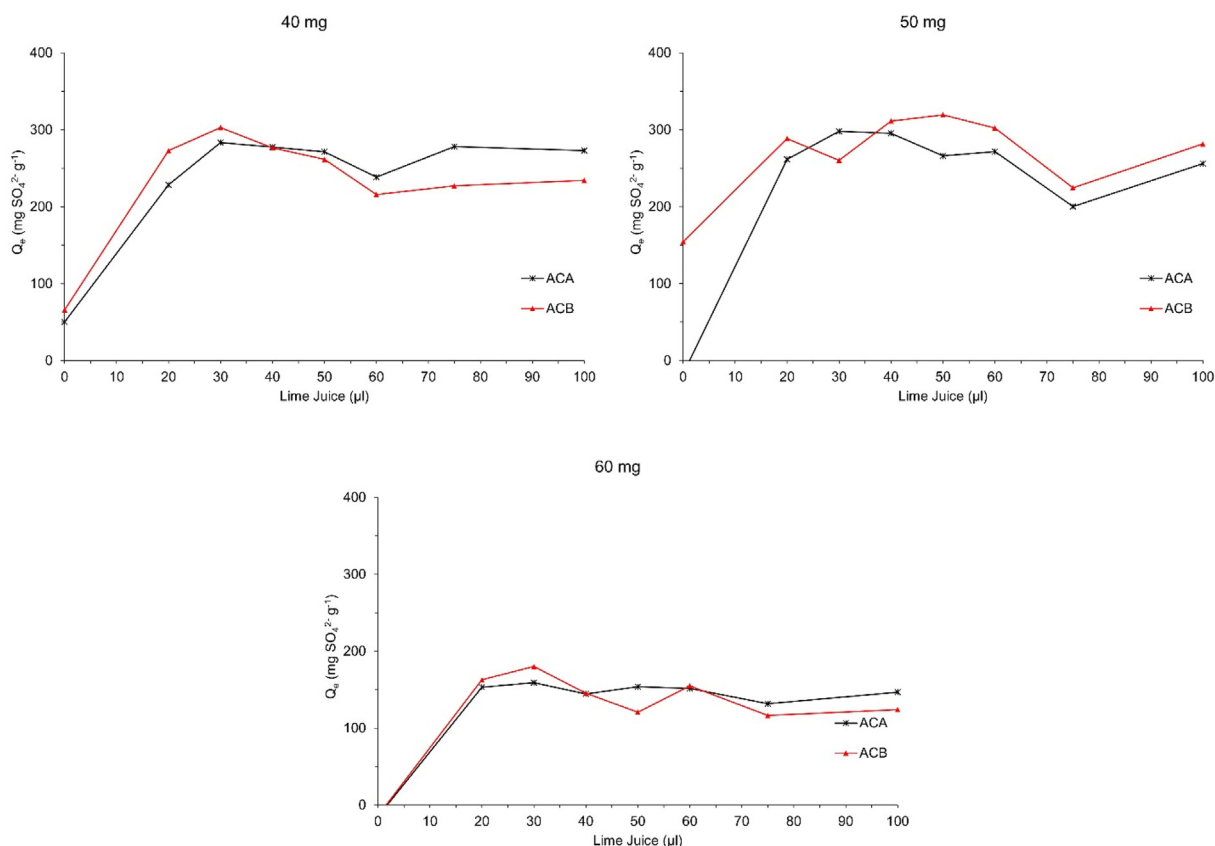
Table 1
The composition of primary ions in the seawater.^a

Ionic constituent	Na ⁺	Ca ²⁺	K ⁺	Mg ²⁺	B ³⁺	Cl ⁻	NO ₃ ⁻	PO ₄ ³⁻	SO ₄ ²⁻
Concentration (mg/L)	8803	370.04	837.2	1183	7.36	19100	0.06	1.75	2555

^a pH 8.12.

Table 2Hydration ratio of ions commonly found in seawater.^a

Ion	F ⁻	Cl ⁻	Br ⁻	NO ₃ ⁻	SO ₄ ²⁻	Na ⁺	K ⁺	Mg ²⁺	Ca ²⁺
Ion radius, nm	0.136	0.181	0.195	0.264	0.290	0.095	0.133	0.065	0.099
Hydrated radius, nm	0.352	0.332	0.330	0.335	0.379	0.358	0.331	0.428	0.412
Hydration ratio	2.59	1.83	1.69	1.27	1.31	3.77	2.49	6.58	4.16

^a Based on the work of Nightingale (1959) and Li et al. (2016).**Fig. 1.** Sulfate ion adsorption capacity with lime juice added for activated carbon dosage of 40, 50, and 60 mg.**Table 3**

Physical and chemical characteristics of the activated carbons.

Activated Carbon	ACA	ACB
BET Surface area (m ² g ⁻¹)	817.811	734.490
BJH Average Pore Size (nm)	1.05702	1.06696
BJH Total Pore Volume (cc/g)	0.432223	0.391835
Ash (%) ^a	0.92	1.85
C (at%)	93.60	95.24
O (at%)	4.81	3.22
N (at%)	ND ^b	ND
pH	6.49	7.34

^a ASTM D2866 method.^b ND: not detected.

influenced by the surface functionality of the carbon material. Specifically, in the case of anion adsorption, such as sulfate ions, the presence of basic carbon surface sites plays a crucial role. These basic sites on activated carbon are associated with the resonating π -electrons of aromatic carbon rings, which have an affinity for protons (Montes-Morán et al., 2004). Basic surface functionalities of activated carbon include oxygen-containing groups with basic characters, such as chromene structures, diketone or quinone groups, and pyrone-like groups (Shafeeyan et al., 2010; Barroso-

Bogeat et al., 2014). Additionally, nitrogen-containing functional groups can also enhance the basicity of activated carbon (Arrigo et al., 2010).

FT-IR spectroscopy was employed to identify the specific basic functional groups present in the activated carbons. The analysis focused primarily on the functional groups relevant to sulfate ion adsorption.

The infrared spectral profiles of ACA and ACB in the range of 450 cm⁻¹ to 4000 cm⁻¹ were compared in Fig. 3. While there were no significant differences overall, ACA exhibited a greater number of peaks corresponding to basic functional groups compared to ACB. These functional groups included chromene, 2-pyrone, aromatic ring, and ketone. Chromene structures with o-disubstituted benzene rings and monosubstituted benzene were observed at 753 cm⁻¹ in ACA and 750 cm⁻¹ in ACB. Both ACA and ACB exhibited a strong band at 1561 cm⁻¹ and 1543 cm⁻¹, respectively, corresponding to the aromatic ring. Additionally, a small peak of ketone was observed at 1719 cm⁻¹ for ACA and 1723 cm⁻¹ for ACB. The vibration signal of 2-pyrone appeared only in ACA, with bands at 1264 cm⁻¹, 1650 cm⁻¹, and 1657 cm⁻¹. The functional groups of 2H-chromene exhibited multiple peaks at 2887 cm⁻¹, 2973 cm⁻¹ for ACA, and 2819 cm⁻¹, 2882 cm⁻¹, and 2965 cm⁻¹ for ACB. The FT-IR spectra also revealed an interaction between

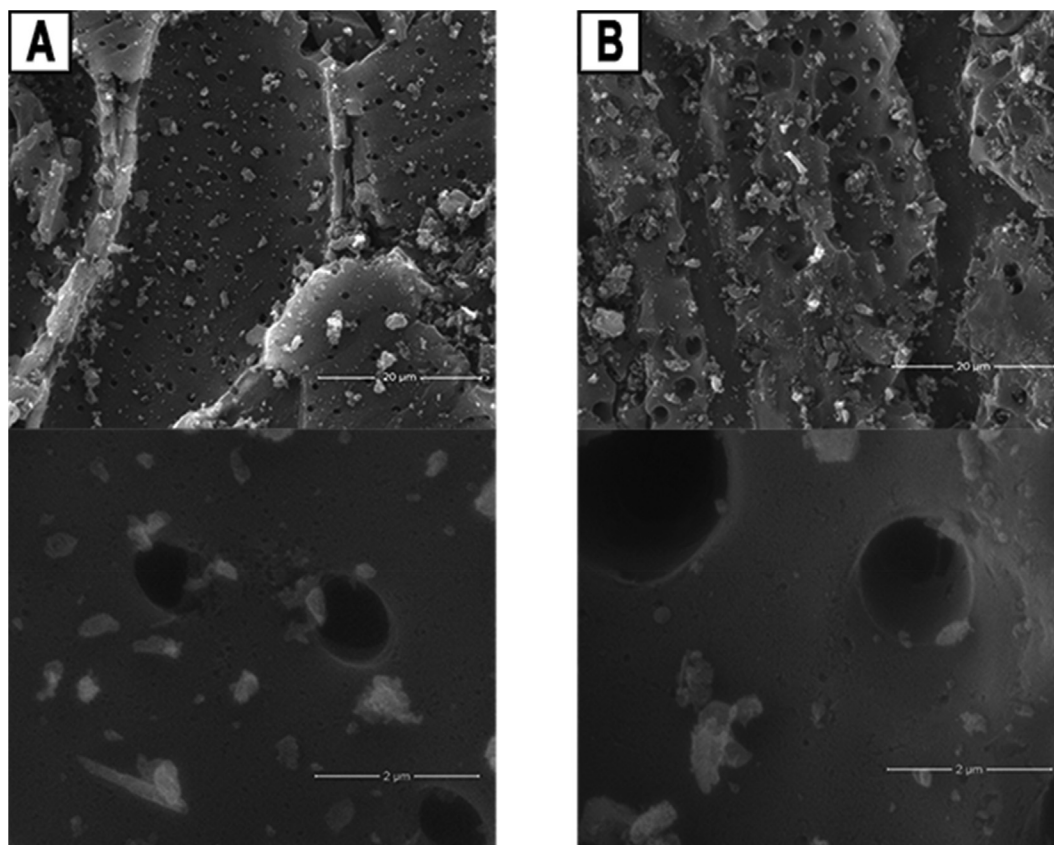


Fig. 2. Micrograph obtained by SEM (A) ACA, (B) ACB.

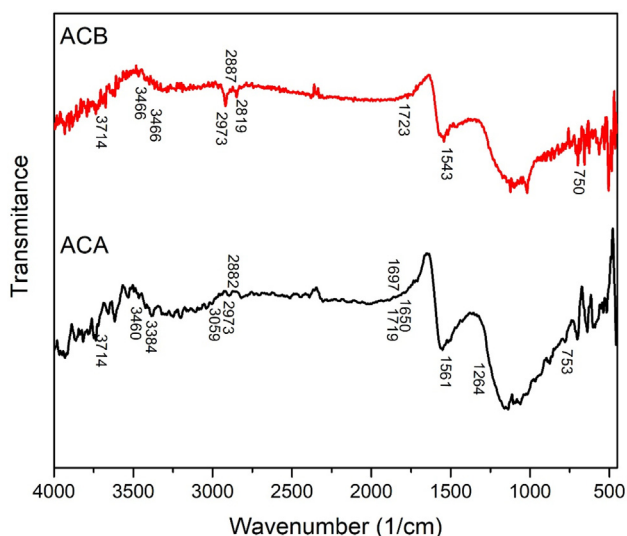


Fig. 3. FTIR Spectrum of AC between 450 and 4000 cm^{-1} .

inorganic compounds and O–H groups, evident as a shoulder peak at 3460 cm^{-1} for ACA and 2366 cm^{-1} for ACB. Furthermore, a single peak at 3714 cm^{-1} was observed in both ACA and ACB samples.

According to the elemental characteristics shown in Table 3, the content of O in ACA is higher than in ACB and the FT-IR analysis shows that ACA has more basic functional groups than ACB. However, the experiment showed that ACB adsorbed sulfate ions better than ACA.

3.5. Lime juice role in sulfate ion adsorption on activated carbon

Although the surface characteristics of the acid-washed activated carbon (ACA) indicated its superiority in terms of pore volume and functional groups, the adsorption capacity of the activated carbon without further treatment (ACB) was higher than that of ACA. This observation could be explained by applying the Hard and Soft Acids and Bases (HSAB) concept to activated carbon, as proposed by Alfarrar et al. (2004).

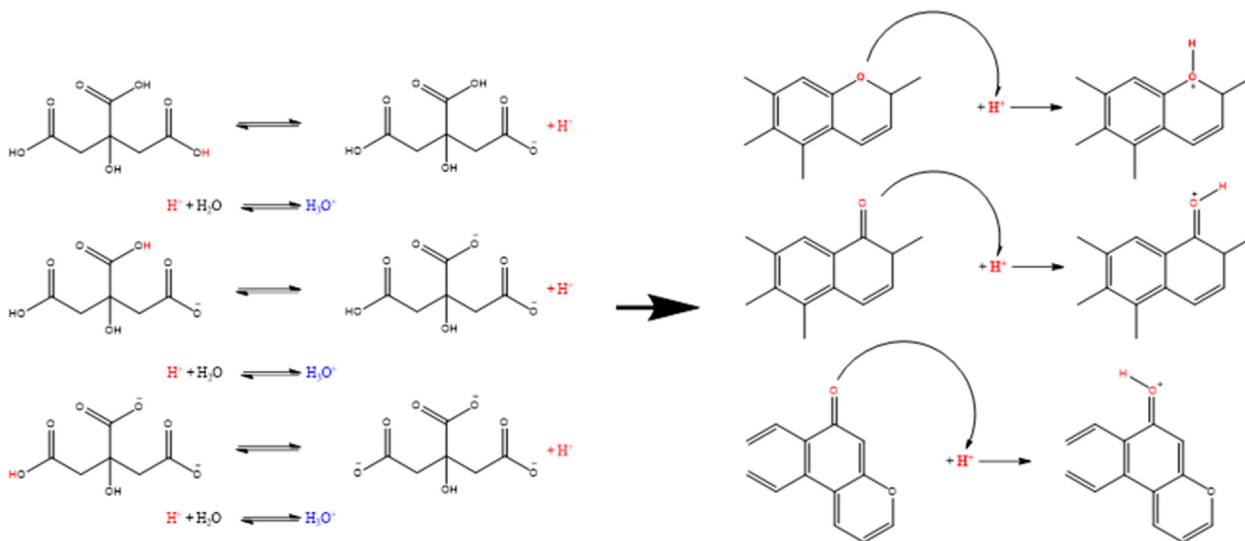
The dominant ions found in seawater, as shown in Table 1, consist of both hard acids and hard bases, and their interactions with the functional groups present on the surface of activated carbon can be explained using the HSAB concept. When seawater is mixed with activated carbon, the functional groups on the carbon surface undergo ionization. The basic functional groups, located at the edges or ends of the carbon basal planes, exhibit high reactivity and initially interact with sulfate ions (Boehm, 2002). However, under normal pH conditions, the adsorption of sulfate ions was minimal in both ACA and ACB. This is likely due to the competition between sulfate ions and coexisting anions, such as chloride, phosphate, and nitrate, for adsorption on the functional groups of activated carbon (Yakout et al., 2017; John et al., 2018). Increasing the dosage of activated carbon introduces more functional groups into the solution, but despite having more basic functional groups, ACA exhibited lower sulfate adsorption compared to ACB.

The addition of lime juice to seawater leads to a decrease in pH, as demonstrated by the average pH values presented in Table 4. The primary source of acidity in limes is the citric acid content, as mentioned by Rangel et al. (2011). Fig. 4 illustrates the ionization process of citric acid and the formation of active sites on activated carbon for basic functionalities in an aqueous solution. The reduction in pH results in the protonation of functional groups,

Table 4

The average pH of seawater solution for each lime juice added.

Lime juice (μl)	0	20	30	40	50	60	75	100
pH (average)	8.12	7.75	7.65	7.52	7.44	7.27	7.04	6.16

**Fig. 4.** The ionization of citric acid and the formation of active sites in activated carbon for basic functionalities (chromene, 2-pyrone and ketone) in aqueous solution.

enabling a greater binding of sulfate ions to these groups. The experimental findings indicate that the adsorption amount of sulfate ions increases with the addition of lime juice, suggesting that sulfate adsorption primarily occurs in the functional groups.

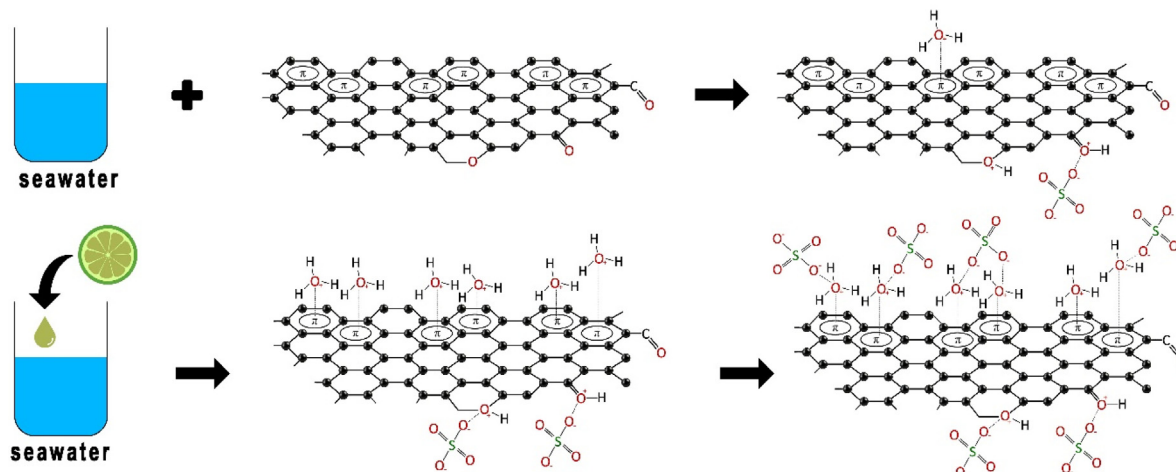
However, despite having a higher number of basic functional groups, ACA exhibited lower performance compared to ACB, as observed in Fig. 1. This phenomenon can be explained by the involvement of basic sites in the carbon basal plane. The basic nature of activated carbon predominantly arises from the delocalized electrons forming bonds within the basal planes. These resonating π -electrons of aromatic carbon rings can interact with positively charged entities, known as cation- π interactions (Ma and Dougherty, 1997; Dougherty, 2012).

Sulfate ions, categorized as hard bases, are not directly attracted to the carbon basal planes. The ionization of basic functional groups and the addition of lime juice result in an increased concentration of hydronium ions in the solution. Through cation- π inter-

actions, the H_3O^+ cations and the carbon surfaces' basal planes establish close-contact structures, where the aromatic rings effectively act as hydrogen bond acceptors (Montes-Morán et al., 1998). ACA, with a higher oxygen content, possesses fewer basal plane sites compared to ACB. Leon et al. (1992) observed that carbons with a small amount of oxygen exhibited an increase in carbon basal planes, which enhance the attraction of hydronium ions. The superior performance of ACB in decreasing sulfate ions can be attributed to its higher carbon basal plane, enabling the bonding of a greater number of hydronium ions to attract sulfate ions. Fig. 5 illustrates the proposed model of sulfate ion adsorption on activated carbon with added lime juice.

3.6. The strength and limitation of the study

The experimental findings indicated that the activated carbon without additional treatment (ACB) outperformed the acid-

**Fig. 5.** The proposed model of sulfate ion adsorption on activated carbon with added lime juice.

washed activated carbon (ACA) in terms of sulfate ion adsorption. Moreover, ACA incurs a higher cost due to the additional acid-washing process. However, it should be noted that the higher adsorption rate in ACB was achieved with increased concentrations of lime juice. Therefore, it is necessary to consider the techno-economic aspects when optimizing the combination of activated carbon type, dosage, and lime juice concentration, as this aspect was not addressed in the current study. Despite this limitation, considering the affordability of activated carbon and limes, this approach may serve as a viable alternative for purifying sea salt.

4. Conclusion

The investigation revealed that the addition of lime juice enhanced the adsorption capacity of sulfate ions from seawater using activated carbon derived from coconut shells. Among the two activated carbons utilized in the study, the untreated activated carbon (ACB) exhibited a higher sulfate ion removal capacity ($320 \text{ mg SO}_4^{2-} \text{ g}^{-1}$) compared to the acid-washed activated carbon (ACA) ($298 \text{ mg SO}_4^{2-} \text{ g}^{-1}$). Lime juice played a crucial role in augmenting the concentration of hydronium ions in the solution. The adsorption of sulfate ions occurred initially at the basic functional groups and subsequently on the carbon basal planes through the presence of hydronium ions. ACB possessed a greater number of basic sites on the carbon basal planes than ACA, which resulted in superior performance in attracting hydronium ions for binding sulfate ions present in seawater.

Funding

This research did not receive any specific grant from funding agencies in the public, commercial, or not-for-profit sectors.

Declaration of Competing Interest

The authors declare that they have no known competing financial interests or personal relationships that could have appeared to influence the work reported in this paper.

Appendix A. Supplementary material

Supplementary data to this article can be found online at <https://doi.org/10.1016/j.jksus.2023.102788>.

References

Alfarra, A., Frackowiak, E., Béguin, F., 2004. The HSAB concept as a means to interpret the adsorption of metal ions onto activated carbons. *Appl. Surf. Sci.* 228, 84–92. <https://doi.org/10.1016/j.apsusc.2003.12.033>.

Álvarez-Merino, M.A., López-Ramón, V., Moreno-Castilla, C., 2005. A study of the static and dynamic adsorption of Zn(II) ions on carbon materials from aqueous solutions. *J. Colloid Interface Sci.* 288, 335–341. <https://doi.org/10.1016/j.jcis.2005.03.025>.

Arrigo, R., Hävecker, M., Wrabetz, S., Blume, R., Lerch, M., McGregor, J., Parrott, E.P.J., Zeitler, J.A., Gladden, L.F., Knop-Gericke, A., Schlögl, R., Su, D.S., 2010. Tuning the acid/base properties of nanocarbons by functionalization via amination. *J. Am. Chem. Soc.* 132, 9616–9630. <https://doi.org/10.1021/ja910169v>.

Barroso-Bogeat, A., Alexandre-Franco, M., Fernández-González, C., Gómez-Serrano, V., 2014. FT-IR analysis of pyrone and chromene structures in activated carbon. *Energy Fuels* 28 (6), 4096–4103. <https://doi.org/10.1021/ef5004733>.

Berry, R.E., 2003. Limes. *Encyclopedia of Food Sciences and Nutrition* (Second Edition).

Boehm, H.P., 2002. Surface oxides on carbon and their analysis: a critical assessment. *Carbon* 40, 145–149. [https://doi.org/10.1016/S0008-6223\(01\)00165-8](https://doi.org/10.1016/S0008-6223(01)00165-8).

Byrne, R.H., 2020. Seawater. *Britannica*. <https://www.britannica.com/science/seawater/> (accessed 26 November 2020).

di Natale, F., Erto, A., Lancia, A., Musmarra, D., 2008. Experimental and modelling analysis of As(V) ions adsorption on granular activated carbon. *Water Res.* 42, 2007–2016. <https://doi.org/10.1016/j.watres.2007.12.008>.

Dougherty, D.A., 2012. The cation- π interaction. *Acc. Chem. Res.* 46 (4), 885–893. <https://doi.org/10.1021/ar300265y>.

Gaya, U.I., Otene, E., Abdullah, A.H., 2015. Adsorption of aqueous Cd(II) and Pb(II) on activated carbon nanopores prepared by chemical activation of doum palm shell. *Springerplus* 4 (1), 1–18. <https://doi.org/10.1186/s40064-015-1256-4>.

Guan, T., Zhao, J., Zhang, G., Zhang, D., Han, B., Tang, N., Wang, J., Li, K., 2018. Insight into controllability and predictability of pore structures in pitch based activated carbon. *J. Micromeso.* 271, 118–127. <https://doi.org/10.1016/j.micromeso.2018.05.036>.

Heydari, A., Arabameri, M., Ebrahimi, A., As'habi, A., Marvdashti, L.M., Yancheshmeh, B.S., Abdolshahi, A., 2020. Determination of magnesium, calcium and sulphate ion impurities in commercial edible salt. *J. Chem. Health Risks* 10 (2), 93–102. <https://doi.org/10.22034/jchr.2020.1883343.1067>.

Hong, S., Cannon, F.S., Hou, P., Byrne, T., Nieto-Delgado, C., 2014. Sulfate removal from acid mine drainage using polypyrrole-grafted granular activated carbon. *Carbon* NY, 73, 51–60. <https://doi.org/10.1016/j.carbon.2014.02.036>.

Hong, S., Cannon, F.S., Hou, P., Byrne, T., Nieto-Delgado, C., 2017. Adsorptive removal of sulfate from acid mine drainage by polypyrrole modified activated carbons: Effects of polypyrrole deposition protocols and activated carbon source. *Chemosphere* 184, 429–437. <https://doi.org/10.1016/j.chemosphere.2017.06.019>.

Hosseini, S.M., Amini, S.H., Khodabakhshi, A.R., Bagheripour, E., Van der Bruggen, B., 2017. Activated carbon nanoparticles entrapped mixed matrix polyethersulfone based nanofiltration membrane for sulfate and copper removal from water. *J. Taiwan Inst. Chem. Eng.* 000 (2017), 1–10. <https://doi.org/10.1016/j.jtice.2017.11.017>.

Ilomuanya, M., Nashiru, B., Ifudu, N., Igwilo, C., 2017. Effect of pore size and morphology of activated charcoal prepared from midribs of *elaeis guineensis* on adsorption of poisons using metronidazole and *escherichia coli* O157:H7 as a case study. *J. Microsc. Ultrastruct.* 5, 32–38. <https://doi.org/10.1016/j.jmau.2016.05.001>.

John, Y., David, V.E., Mmereki, D., 2018. A comparative study on removal on hazardous anions from water by adsorption: A review. *Int. J. Chem. Eng.* 2018, 3975948. <https://doi.org/10.1155/2018/3975948>.

Koehlert, K., 2017. Activated carbon: Fundamentals and new applications. *Chemical Engineering*. Juli 2017. <https://www.chemengonline.com/activated-carbon-fundamentals-new-applications/> (accessed 20 July 2020).

Leon, C.A., Leon, Y., Solar, J.M., Calemme, V., Radovic, L.R., 1992. Evidence for protonation of basal plane sites on carbon. *Carbon* 30 (5), 797–811. [https://doi.org/10.1016/0008-6223\(92\)90164-R](https://doi.org/10.1016/0008-6223(92)90164-R).

Li, Y., Zhang, C., Jiang, Y., Wang, T., Wang, H., 2016. Effects of hydration ratio on the electrosorption selectivity of ions during capacitive deionization. *Desalination* 399, 171–177. <https://doi.org/10.1016/j.desal.2016.09.011>.

Ma, J.C., Dougherty, D.A., 1997. The cation- π interaction. *Chem. Rev.* 97, 1303–1324. <https://doi.org/10.1021/cr9603744>.

Masuzawa, T., 1980. Impurities contained inside the crystal of solar and vacuum evaporated salts. *Fifth International Symposium on Salt* 2, 463–473.

Miyazato, T., Nuryono, N., Kobune, M., Rusdiansar, B., Otomo, R., Kamiya, Y., 2020. Phosphate recovery from an aqueous solution through adsorption desorption cycle over thermally treated activated carbon. *J. Water Process Eng.* 36, <https://doi.org/10.1016/j.jwpe.2020.101302>.

Montes-Morán, M.A., Angel Menéndez, J., Fuente, E., Suárez, D., 1998. Contribution of the basal planes to carbon basicity: an ab initio study of the H_3O^+ - π interaction in cluster models. *J. Phys. Chem. B* 102 (29), 5595–5601. <https://doi.org/10.1021/jp972656t>.

Montes-Morán, M.A., Suárez, D., Menéndez, J.A., Fuente, E., 2004. On the nature of basic sites on carbon surfaces: An overview. *Carbon* 42, 1219–1225. <https://doi.org/10.1016/j.carbon.2004.01.023>.

Nightingale, E.R., 1959. Phenomenological theory of ion solvation. Effective radii of hydrated ions. *J. Phys. Chem.* 63 (9), 1381–1387. <https://doi.org/10.1021/j150579a011>.

Penniston, K.L., Nakada, S.Y., Holmes, R.P., Assimios, D.G., 2008. Quantitative assessment of citric acid in lemon juice, lime juice and commercially-available fruit juice products. *J. Endourol.* 22 (3), 567–570. <https://doi.org/10.1089/end.2007.0304>.

Rahmati, M., Yeganeh, G., Esmaeili, H., 2019. Sulfate ion removal from water using activated carbon powder prepared by *ziziphus spina-christi* lotus leaf. *Acta. Chim. Slov.* 66, 888–898. <https://doi.org/10.17344/acsi.2019.5093>.

Rangel, C.N., Carvalho, L.M.J., Fonseca, R.B.F., Soares, A.G., Jesus, E.O., 2011. Nutritional value of organic acid lime juice (*Citrus latifolia* T.), cv. Tahiti. *Food Sci. Technol. (Campinas)* 31 (4), 918–922. <https://doi.org/10.1590/S0101-20612011000400014>.

Runtti, H., Tuomikoski, S., Kangas, T., Kuokkanen, T., Rämö, J., Lassi, U., 2016. Sulfate removal from water by carbon residue from biomass gasification: Effect of chemical modification methods on sulfate removal efficiency. *BioResources* 11 (2), 3136–3152. <https://doi.org/10.15376/biores.11.2.3136-3152>.

Sedivy, V.M., 2009. Environmental balance of salt production speaks in favour of solar saltworks. *Glob. NEST J.* 11 (1), 41–48.

Shafeeyan, M.S., Daud, W.M.A.W., Houshmand, A., Shamiri, A., 2010. A review on surface modification of activated carbon for carbon dioxide adsorption. *J. Anal. Appl. Pyrolysis* 89, 143–151. <https://doi.org/10.1016/j.jaap.2010.07.006>.

Shen, W., Li, Z., Liu, Y., 2008. Surface chemical functional groups modification of porous carbon. *Recent Pat. Chem. Eng.* 1 (1), 27–40. <https://doi.org/10.2174/1874478810801010027>.

Sun, J., Liua, X., Duan, S., Alsaedi, A., Zhang, F., Hayat, T., Li, J., 2018. The influential factors towards graphene oxides removal by activated carbons: Activated

- functional groups vs BET surface area. *J. Mol. Liq.* 271, 142–150. <https://doi.org/10.1016/j.molliq.2018.08.118>.
- Waghaye, S.Y., Kshirsagar, R.B., Sawate, A.R., Shareef, M., 2019. Studies on physical and chemical composition of lime (*Citrus aurantifolia* L.). *Int. J. Chem. Stud.* 7 (2), 1098–1100.
- Wong, K.V., 2016. Salt of Our Lives. *J. Epidemiol. Pub. Health Rev.* 1 (2), 1–3. <https://doi.org/10.16966/2471-8211.114>.
- Yakout, S.M., Salem, N.A., Mostafa, A.A., Abdeltawab, A.A., 2017. Relation between biochar physicochemical characteristics on the adsorption of fluoride, nitrite, and nitrate anions from aqueous solution. Part. *Sci. Technol.* 37 (1), 118–122. <https://doi.org/10.1080/02726351.2017.1352633>.
- Zhu, M., Yin, X., Chen, W., Yi, Z., Tian, H., 2019. Removal of sulphate from mine waters by electrocoagulation/rice straw activated carbon adsorption coupling in a batch system: Optimization of process via response surface methodology. *J. Water Reuse Desalin.* 9 (2), 63–172. <https://doi.org/10.2166/wrd.2018.054>.